Phase Retrieval of Gyrotron Beams Based on Irradiance Moments

James P. Anderson, Michael A. Shapiro, Richard J. Temkin, *Fellow, IEEE,* and Douglas R. Denison

***Abstract*—We present the formulation of the moment method applied to the determination of phase profiles of microwave beams from known amplitudes. While traditional approaches to this problem employ an iterative error-reduction algorithm, the irradiance moment technique calculates a two-dimensional polynomial phasefront based on the moments of weighted intensity measurements. This novel formulation has the very important advantage of quantifying measurement error, thus allowing for its possible reduction. The validity of the irradiance moment approach is tested and confirmed by examining a simple case of an ideal Gaussian beam with and without measurement errors. The effectiveness of this approach is further demonstrated by applying intensity measurements from cold-test gyrotron data to produce a phasefront solution calculated via the irradiance moment technique. The accuracy of these results is shown to be comparable with that obtained from the previously developed iteration method.**

***Index Terms*—Gaussian beam, gyrotron, irradiance moments, phase retrieval.**

I. Introduction

MICROWAVES generated from a gyrotron in high-order waveguide modes must be transformed into a low-order symmetrical mode for transmission and application. Either a Vlasov launcher [1] or its modification, a rippled-wall Denisov launcher [2], radiates the microwave energy extracted from bunched electrons. The microwave beam is then shaped and directed using a series of internal mode converter reflectors comprised of phase correctors and simple focusing mirrors. The configuration shown in Fig. 1, which represents the layout of a 1-MW 110-GHz gyrotron [3], uses a system of two doubly-curved reflectors ($M1$ and $M2$) and two phase-correcting reflectors ($M3$ and $M4$) [4]. After the resultant beam propagates through the output window, the beam typically undergoes additional phase correction and/or focusing to further convert it to a Gaussian beam. Gaussian beams are advantageous since they may be focused and redirected using simple optical components. Additionally, the beam profile of a Gaussian beam matches well with the fundamental HE_{11}-mode profile in a corrugated waveguide.

Manuscript received February 18, 2001; revised May 23, 2001. This work was supported in part by the U.S. Department of Energy, by the Office of Fusion Energy Sciences, and by the Virtual Laboratory for Technology.

J. P. Anderson, M. A. Shapiro, and R. J. Temkin are with the MIT–Plasma Science and Fusion Center, Massachusetts Institute of Technology, Cambridge, MA 02139 USA (e-mail: janders@mit.edu; shapiro@psfc.mit.edu; temkin@psfc.mit.edu).

D. R. Denison was with the MIT–Plasma Science and Fusion Center, Massachusetts Institute of Technology, Cambridge, MA 02139 USA. He is now with the Signature Technology Laboratory, Georgia Institute of Technology, Atlanta, GA 30332 USA (e-mail: doug.denison@gtri.gatech.edu).

Publisher Item Identifier S 0018-9480(02)05200-6.

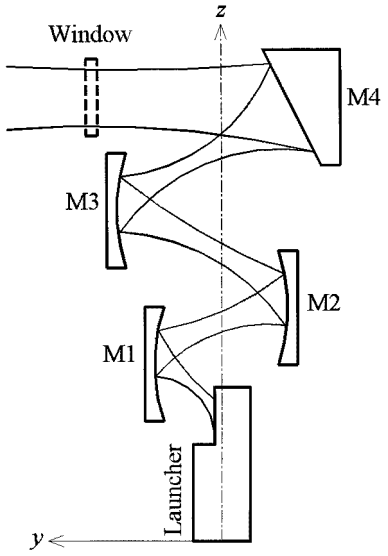

Fig. 1. Gyrotron internal-mode converter schematic.

A common approach to design the phase correctors is to use either analytical or numerical techniques to approximate the radiation pattern emitted from the launcher. Attempts have been made, for example, to model the radiated fields generated from the rippled-wall launcher [5]. However, experimental results have shown that the measured field profile does not agree with predicted beam behavior at the gyrotron window [3]. The discrepancies between theory and experiment may occur from problems with launcher alignment or from problems with the launcher theory itself.

To fully account for the field radiated from the internal mode converter, cold-test intensity measurements are taken initially, without the presence of an electron beam in vacuum, using a high-order mode generator. The low-power quasi-optical microwave beam radiated from the launcher can be used to design the correcting mirrors. These mirror designs, however, require knowledge of the free-space propagation behavior of the beam, characterized by both the amplitude and phase. While the amplitude profile can be directly measured at low power using a spatial scanner with a receiving horn and detector, the phasefront (at frequencies above 100 GHz) cannot be so easily determined. Therefore, numerical methods are ordinarily employed to retrieve the phase based on a series of measured intensity data taken at several planes located past the launch point. Fig. 2 shows a schematic of a cold-test gyrotron experimental setup, which may be used to design appropriate external phase-correcting mirrors. A series of measurement planes, shown as

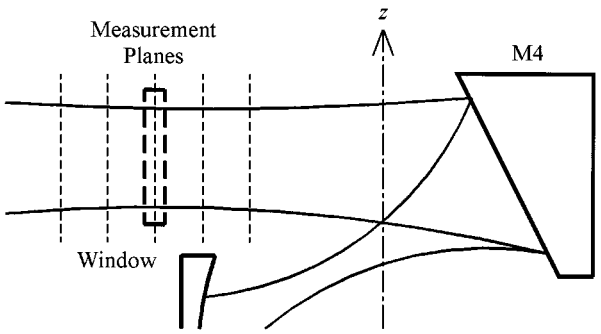

Fig. 2. Cold-test measurement plane schematic near the location of the gyrotron window.

dotted lines, lie immediately before and after the window location where the beam is the narrowest (the beam waist) [6]. In the actual cold test, the window is omitted from the setup. Examples of discretely sampled measured data on a series of planes are presented in Section V. Alternatively, in the hot test, in which high-power microwaves are generated from an electron beam, data can be taken on a series of planes beyond the window plane with an infrared camera viewing a microwave absorbing screen.

Several methods have been developed to retrieve the microwave output phase based on intensity measurements. The more traditional approach, based on the Gerchberg–Saxton formulation [7], uses an iterative algorithm. This method attempts an initial approximation of the phase at the first measurement plane and then propagates this paraxial beam forward to the next measurement plane using a Fourier transform inter-plane wave propagation routine [8]. Using the assumed phase of the resultant beam with the measured intensity at this plane, the beam is then propagated back to the initial plane. The initial phase approximation is then modified to compensate for the error between the measured and reconstructed amplitudes [9], [10]. Through numerous repetitions the phase solution generally converges until the amplitude error is minimized [10], [11]. This error-reduction approach, known as the iteration method (or "phase-retrieval method"), although numerically intensive, has proven to be successful in designing accurate internal phase correcting mirrors [6], [12] and external mirrors [12]–[14].

An added advantage of using intensity measurements is the valuable information gained from computing the normalized weighted moments, or expectation values. The moments are useful to improve the reliability of the data and for phase retrieval, especially when the data set is taken using an infrared camera in hot tests, since phase-retrieval methods are typically sensitive to misalignment. Since measurements at different planes require moving the camera and target, alignment errors are not uncommon. Moreover, the work space is typically limited, which forces frequent repositioning of the system. In [15], the moments of infrared images of gyrotron radiation were calculated to determine the accuracy of the spatial alignment of the images. The iterative phase-retrieval procedure and internal mirror synthesis [6] were employed using only the well-aligned images.

A phase-retrieval algorithm based solely on these moments may prove to yield even more accurate results while being computationally more efficient [16]. This "irradiance moment" approach assumes an initial two-dimensional (2-D) polynomial phasefront, which is predominately parabolic, but with additional higher order phase aberrations. The coefficients of the polynomial are calculated from the weighted moments based on intensity distributions over several measurement planes. Although employed in optics for applications such as characterizing the beam quality of high-power multimode lasers [17], this numerical method, to our knowledge, has never before been applied to the phase retrieval of a microwave beam. The microwave problem is recognized as more difficult than optical applications because of diffraction.

In the following sections, the theory behind the irradiance moment technique will be briefly presented, along with the generalized approach for retrieving the phase. The success of this scheme is then demonstrated numerically using both a simple Gaussian beam and previously generated gyrotron cold- test data. The final section will discuss future developments for the irradiance moment technique.

II. Phase-Retrieval Based on Moment Techniques

The basic idea behind any phase-retrieval method is to determine the initial phase from intensity measurements near the beam waist. While commonly used Gerchberg–Saxton iteration methods rely on repeatedly improving an initial phase approximation to reduce amplitude error [9], the irradiance moment technique attempts to solve the initial phase polynomial coefficients from the weighted moments. Both approaches make use of Fresnel diffraction theory to propagate the beam, assuming the beam is linearly polarized and propagates paraxially. However, the iteration method advances the amplitude and phase of the beam, whereas the irradiance moment technique propagates the moments of the beam. Using the moment approach, we present the relationship between the phase at a fixed plane and irradiance moments propagating orthogonally from this plane. Although this relationship is generally nonlinear, we may form a set of solvable relations from the linear terms of the moments. After calculating the moments and predicting how they propagate, we then apply these linear relations to determine the phase.

To be consistent with the geometry shown in Figs. 1 and 2, we will assume the paraxial beam propagates along the y-direction. The z-axis is reserved as the axis of the gyrotron. The behavior of the wave at a particular axial location y, which includes amplitude A_y and phase Φ_y, can be described by its wave function, or complex amplitude ψ, where $\psi(x,y,z) = A_y(x,z)e^{i\Phi_y(x,z)}$.

The moments of the wave function are based on the normalized weighted intensity integrated over the finite measurement plane at an axial location y. They are defined as

$$M_{pq}(y) = \langle x^p z^q \rangle_y = \int\int x^p z^q A_y^2(x,y)\,dx\,dz \qquad (1)$$

where the integration is performed over all x's and z's.

It is important to note that a numerical approximation of the irradiance moment technique (and, indeed, of any phase-retrieval method relying on intensity measurements) must be made from the fact that the measurement planes are finite. Theoretically, the moments are calculated by integrating over an infinite plane. For the integrals in the irradiance moment

technique to be completely accurate, the amplitude at the plane edges must be zero. In practice, beam information outside of the plane limits is lost. This truncation introduces an error into the calculation of the moments, particularly higher order moments. For example, if a Gaussian beam is truncated to 20 dB below the peak value, then the error in the fourth-order moments is over 10%. If the measurements are truncated to 28 dB, this error decreases to 2%. Of course, if the measurement plane is chosen very large, such that the truncation is at 35 dB, then the fourth-order moment error is a very small number, around 0.5%.

The Kirchhoff–Huygens diffraction integral in its Fresnel approximation describes a paraxial beam at any distance in terms of the initial wave function [18]

$$\psi(x,y,z) = \frac{i}{\lambda y}\int\int dx'\,dz'\left[\psi(x',0,z') \times \exp\left(-i\frac{k\left[(x'-x)^2+(z'-z^2)\right]}{2y}\right)\right] \tag{2}$$

where λ is the wavelength and $k = 2\pi/\lambda$ is the wavenumber. By applying the definition of moments [see (1)] to the diffraction integral, we can show how the moments change as the beam propagates [19], [20] as follows:

$$M_{pq}(y) = \left(-i\frac{y}{k}\right)^{p+q}\int\int dx\,dz\left[\psi(x,0,z) \times \exp\left(-i\frac{k(x^2+z^2)}{2y}\right)\right] \times \frac{\partial^p}{\partial x^p}\frac{\partial^q}{\partial z^q}\left[\psi^*(x,0,z)\exp\left(i\frac{k(x^2+z^2)}{2y}\right)\right] \tag{3}$$

where $\psi(x,0,z) = A_0(x,z)e^{i\Phi_0(x,z)}$ is the analytic complex amplitude at the initial $(y = 0)$ plane and $\psi^*(x,0,z)$ is its complex conjugate. This formula yields an expression for the propagation behavior of the moments. Furthermore, it relates the moments at any given axial location to the initial phase. Explicit expressions are listed in the Appendix for the first- and second-order moments.

From (3), the moment $M_{pq}(y)$ is, in general, a one-dimensional polynomial along the direction of propagation y with order $p+q$ and coefficients $C_{pq}^{(m)}$ as follows:

$$M_{pq}(y) = M_{pq}(0) + \sum_{m=1}^{p+q} C_{pq}^{(m)} y^m = \sum_{m=0}^{p+q} C_{pq}^{(m)} y^m. \tag{4}$$

The moment polynomial coefficients $C_{pq}^{(m)}$ are determined by a combination of the initial amplitude and phase and their derivatives integrated over the measurement plane. In practice, the data set is analyzed by finding a series of M_{pq} values at several planes along y. The calculated M_{pq} values are then applied to a one-dimensional polynomial fit in y to obtain the moment polynomial coefficients $C_{pq}^{(m)}$ up to $m = p+q$, the polynomial order. This technique is illustrated in Section IV.

From (3) and (4), we can show that the linear coefficient of any moment order M_{pq}, which measures the slope of the moment at the retrieval plane, may be expressed as a product of the initial intensity and weighted initial phase derivative integrated over the xz-plane

$$C_{pq}^{(1)} = -\frac{1}{k}\int\int dx\,dz\left[\frac{\partial\Phi_0}{\partial x}\frac{\partial}{\partial x}(x^p z^q) + \frac{\partial\Phi_0}{\partial z}\frac{\partial}{\partial z}(x^p z^q)\right]A_0^2. \tag{5}$$

A set of linear equations may be created from the linear moment coefficients by assuming an appropriate form for the phasefront. For a spatially directed microwave beam, the phasefront can be expanded as a 2-D polynomial at the reference transverse (xz)-plane with coefficients ϕ_{ij}

$$\Phi_0(x,z) = \phi_{10}x + \phi_{01}z + \phi_{20}x^2 + \phi_{11}xz + \phi_{02}z^2 + \phi_{30}x^3 + \ldots. \tag{6}$$

The series in (6) converges for beams decaying exponentially in the transverse direction. One way to show this is by applying the uniform stationary phase method [21].

The linear moment coefficients $C_{pq}^{(1)}$ are linear functions of the phase expansion coefficients and the initial amplitude moments, represented here as the intercept coefficients $C_{pq}^{(0)}$, where $C_{pq}^{(0)} = M_{pq}(0)$. This linear dependence is shown in the example provided in the Appendix. Linearized equations are formed because, from (5) and the selection of a suitable polynomial phasefront expansion, the slope of each moment propagating in y is linear with respect to the phase expansion coefficients in the transverse (xz)-plane.

The phasefront expansion of Φ_0 must be truncated to form a set of solvable linear equations from the expressions relating the linear moment coefficients to the phase coefficients. This approximation is valid due to the fact that the gyrotron beam is directed and paraxial. For well-behaved paraxial beams, the phasefront described by (6) is primarily parabolic and nearly symmetrical. Therefore, the ϕ_{02} and ϕ_{20} coefficients are the dominant terms in the polynomial phasefront expansion. Higher order aberrations are included to provide an accurate phasefront solution. Generally, the solution is more accurate if many phase expansion terms are included. As mentioned earlier, however, the series in (6) will converge for directed beams. Only the first few higher order phase expansion terms are necessary to provide an accurate solution.

The set of equations is closed and solvable by requiring that the maximum moment order of the calculated linear C_{pq} coefficients or $C_{pq}^{(1)}$ be equal to the order of the truncated 2-D transverse plane phase expansion in Φ_0, which is defined as N. In other words, $(p+q)_{\max} = (i+j)_{\max} = N$. The number of equations that are formed is simply the summation of the number of unknown phase expansion coefficients. Since each $(i+j)$th expansion in Φ_0 has $i+j+1$ coefficients

$$\text{Number of Equations} = \sum_{n=1}^{N}(n+1) = \frac{N(N+3)}{2}. \tag{7}$$

The phase is calculated by first truncating the phasefront at the initial plane Φ_0 to order N, which specifies the number of phase expansion coefficients ϕ_{ij}. The moments $M_{pq}(y)$ are directly calculated from intensity measurements at several planes y for every p and q up to $p+q=N$. Each of these moments is then fitted over y to a one-dimensional polynomial of order $p+q$ to determine the moment coefficients $C_{pq}^{(m)}$ up to $m=p+q$. Only the linear coefficients $C_{pq}^{(1)}$ and the coefficients of zero rank $C_{pq}^{(0)}$, which represent the slope and moment intercept, respectively, are required to form a series of linear equations, which ultimately determine the phase expansion coefficients.

Since each of the moments is fitted over y to polynomials of order $p+q$, the number of planes (y data) required by the irradiance moment technique must be at least $p+q+1$. Since $(p+q)_{\max}=(i+j)_{\max}=N$, then the minimum number of planes is $N+1$ for an Nth order 2-D polynomial phasefront solution. More data planes may be used to insure a better moment fit and, thus, a more accurate solution. If fewer planes are used, however, the solution is indeterminate and an erroneous solution may occur. Since there will not be enough data in this instance to fit to the moment polynomials, the solution will not be unique.

After the phasefront has been determined at the initial plane, external reflectors may be designed to correct for the phase and amplitude of the gyrotron output, and to effectively couple power to the fundamental HE_{11} mode of a corrugated waveguide for guided transmission. In the procedure of reflector synthesis, we can take advantage of the irradiance moment-method approach's phasefront solution, which is in analytical form. Therefore, the numerical procedure of phase unwrapping, required for reflector synthesis using the iteration method [6], is not needed using irradiance moments. This improves the mirror shaping because phase unwrapping is ambiguous.

III. Outline of the Irradiance Moment Approach

The procedure for finding a unique phasefront solution using the irradiance moment technique is fairly straightforward. The general steps for finding an Nth order unique phase solution is as follows.

- Step 1) Normalize all the measured intensity planes such that $M_{00}(y)=1$ at each y location.
- Step 2) Calculate the moment $M_{pq}(y)$ numerically at each plane, including the initial plane $(y=0)$ by applying a discrete integration routine to the weighted amplitude data.
- Step 3) Generate a one-dimensional polynomial fit in y of order $p+q$ for the M_{pq} moment.
- Step 4) Repeat steps 2 and 3 for each moment M_{pq} up to $p+q=N$.
- Step 5) Propagate the moments analytically by applying Fresnel diffraction theory. Specifically, the linear moment coefficients $C_{pq}^{(1)}$ must be expressed in terms of the initial phase [see (5)].
- Step 6) Expand and truncate the initial phasefront Φ_0 as an Nth order 2-D polynomial in the xz-plane.
- Step 7) Find a linear analytical expression for each of the linear moment coefficients $C_{pq}^{(1)}$ from step 5 in terms of the phase expansion coefficients ϕ_{ij} from step 6 and the moments at the initial plane $M_{pq}(0)$ represented by $C_{pq}^{(0)}$.
- Step 8) Solve the set of linear equations for the phase expansion coefficients ϕ_{ij} using the moment coefficients from the polynomial moment fits in y.

IV. Irradiance Moment Results: Technique Gaussian Beam

A. Ideal Gaussian Beam

The advantages and limitations of the irradiance moment approach are demonstrated by testing the algorithm with both an ideal Gaussian beam and a series of existing measured gyrotron intensity data. The results obtained from the iteration method are also presented for comparison.

For the ideal Gaussian case, a beam is chosen with $\lambda=0.273$ cm and a waist w_0 of 2.0 cm at $y=0$. Five planes containing discretized ideal Gaussian amplitude data are generated for the phase-retrieval calculations at $y=20,30,40,50$, and 60 cm. After the phase is retrieved at the initial plane $y=20$ cm, the amplitude and computed phase are propagated to an observation plane $y=-30$ cm. A propagation routine based on the 2-D discretized fast Fourier transform calculates the beam wave function at any axial location given the initial amplitude and phasefront solution. The reconstructed complex amplitude at the observation plane may then be compared with the theoretical Gaussian amplitude and phase.

Since five amplitude planes are used in the irradiance moment technique phase-retrieval algorithm, it is possible to assume a fourth-order phasefront 2-D polynomial at the initial $y=20$ cm plane. However, this expansion is not necessary since the phasefront of an ideal Gaussian beam is parabolic and will not contain higher order aberrations. A second-order phasefront polynomial $(N=2)$ is more appropriate for the calculations. A set of five linear equations [see (7)] based on the five first- and second-order moments are required to solve the unknown phase coefficients $\phi_{10},\phi_{01},\phi_{20},\phi_{11}$, and ϕ_{02}. These equations are derived explicitly in the Appendix. Note that this algorithm in principle requires only three data planes since $N=2$. Five planes are included to provide more data with which to accurately fit the moments and to be consistent with the other example in this section.

To understand how the irradiance moment approach works in this simple Gaussian case, we must examine the behavior of the moments. The first-order moments M_{10} and M_{01} are measures of the expectation values or $\langle x\rangle$ and $\langle z\rangle$, respectively. They indicate where the center of the beam is located. For the ideal Gaussian case, they are at zero for all planes since the beam does not drift. The values of the linear polynomial coefficients are zero everywhere, i.e., the slopes are zero $(C_{10}^{(1)}=C_{01}^{(1)}=0)$ and the intercepts are zero $(C_{10}^{(0)}=C_{01}^{(0)}=0)$.

The second-order moments M_{20},M_{11}, and M_{02} are not as simple to understand. Physically, these moments represent the size of the beam in x and z. For a symmetric beam, $M_{11}=$

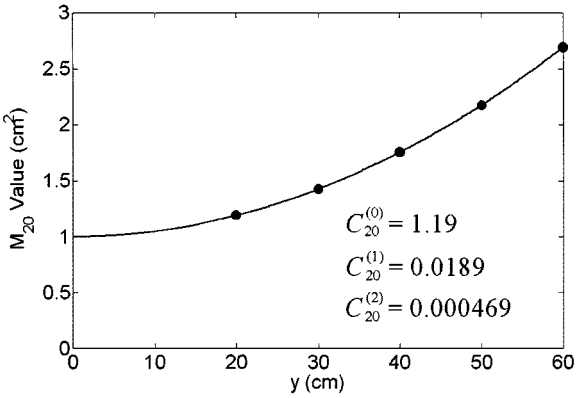

Fig. 3. Second-order M_{20} moments are fitted to a quadratic in y. The coefficients of the fit originated at the retrieval plane ($y = 20$ cm) are listed in the plot.

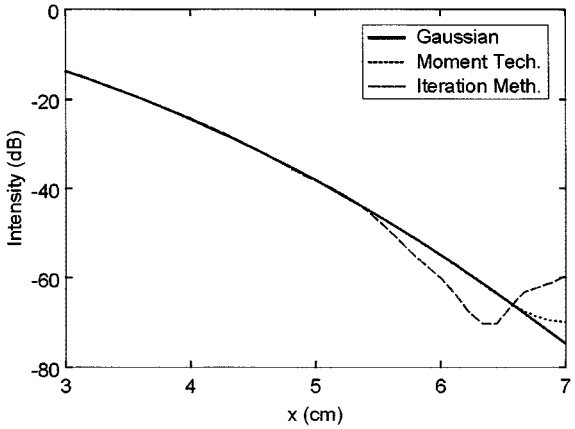

Fig. 4. Mid-plane ideal Gaussian intensity profile at the observation plane ($y = -30$ cm) is compared with the reconstructed amplitudes using the iteration method and irradiance moment technique near the edge of the beam.

0 everywhere since there is no coupling between x and z. The coefficients for this moment polynomial ($C_{11}^{(0)}, C_{11}^{(1)}$, and $C_{11}^{(2)}$) are zero. The other second-order moments M_{20} and M_{02} follow a quadratic describing the beam growth over distance. The calculated M_{20} moments at each of the five planes are shown in Fig. 3. Note the predicted M_{20} moment value at $y = 0$ cm is 1.0 cm, which accurately reflects the beam waist ($w_0 = 2.0$ cm).

As seen in the example in Fig. 3, the polynomial coefficients of each moment at the phase-retrieval plane ($y = 20$ cm) are easily determined. Recall only $C_{pq}^{(0)}$ and $C_{pq}^{(1)}$ are needed to calculate the phasefront.

The irradiance moment 2-D phasefront solution that uses the fitted moment coefficients in the set of five linear equations is $\phi_{10} = \phi_{01} = 0, \phi_{20} = \phi_{02} = 0.0914\ \text{cm}^{-2}$, and $\phi_{11} = 0$. The calculated phasefront at $y = 20$ cm has the form

$$\Phi_0(x,z) = \left(0.0914\ \text{cm}^{-2}\right)x^2 + \left(0.0914\ \text{cm}^{-2}\right)z^2. \quad (8)$$

From the radius of curvature formula based on the theory of Gaussian optics, the phasefront should have the following solution:

$$\phi_{20} = \phi_{02} = \frac{2ky}{4y^2 + \left(kw_o^2\right)^2}. \quad (9)$$

Evaluating this expression at $y = 20$ cm using the given beam parameters yields $\phi_{20} = \phi_{02} = 0.0914\ \text{cm}^{-2}$. Therefore, by testing the moment method with artificial Gaussian beam data, we have verified that the irradiance moment technique produces an accurate solution for this simple example.

The intensity at the observation plane ($y = -30$ cm) was reconstructed using the phasefront computed by the irradiance moment approach, as described above. In addition, we obtained a phasefront solution by applying the iteration method algorithm to the artificial Gaussian data. The reconstructed intensity based on this converged solution was also calculated at the observation plane. The results of both methods are compared in Fig. 4. Both algorithms accurately reconstruct the amplitude, although the irradiance moment approach produces a more accurate beam below −40 dB. This is not surprising since the iteration method attempts to reduce the error below an acceptable tolerance level, whereas the moment method provides a more exact one-step numerical solution.

B. Gaussian Beam With Uncorrected Offset Measurement Error

While the ideal Gaussian case confirms the validity of the irradiance moment approach, it is a trivial exercise. More insight may be gained from manufacturing a simple case where measurement error has occurred. Errors in the form of shifted or offset data are common when using laboratory devices such as an infrared camera to measure intensity. It is important, therefore, to examine how such an error affects the phase-retrieval process.

To examine offset error, the same five planes containing ideal Gaussian amplitude data are used as in the previous example. Error is introduced at the $y = 40$ cm plane, where the beam is shifted in the x-direction by $+0.7$ cm, a distance greater than two wavelengths. Such a shift is not physical since the beam must travel in a straight line, yet the error could occur in an experiment if an infrared camera and viewing screen were misaligned. As before, a second-order polynomial phasefront form is solved at the initial $y = 20$ cm plane.

Since the beam is shifted, $M_{10}(y)$ is zero for all y, except at $y = 40$ cm, where $M_{10}(40\ \text{cm}) = 0.7$ cm. The best linear fit of the first-order M_{10} or $\langle x \rangle$ moment is also shifted to reflect the increased average value over all five M_{10} moments. Therefore, while the $C_{10}^{(1)}$ coefficient or slope does not change, the $C_{10}^{(0)}$ value is raised slightly to the averaged value of the M_{10} moments, i.e., 0.14 cm. Since there is no shift in the z-direction, $M_{01}(y)$ is still zero everywhere.

Since the introduction of an offset error does not change the size of the beam, the second-order moments are exactly the same as before. The M_{20} moments, for example, follow a smooth quadratic with or without an offset in the data (Fig. 3). The $C_{20}^{(0)}$ and $C_{20}^{(1)}$ coefficients that are determined from this fit do not change.

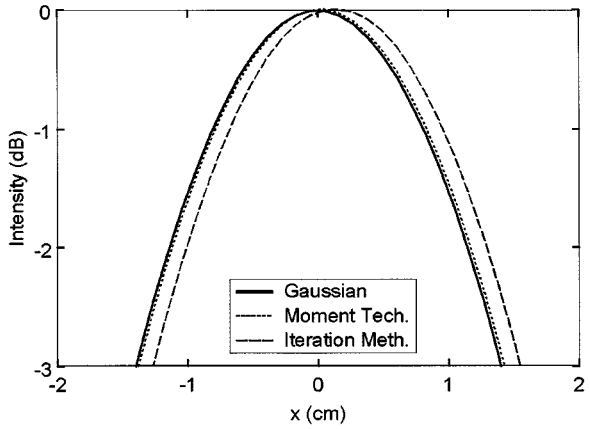

Fig. 5. Intensity profiles near $x = 0$ at the observation plane reconstructed from the irradiance moment technique and the iteration method for the case where offset measurement error has occurred at the $y = 40$ cm plane.

The phasefront solution computed from the set of equations using the artificial data with offset becomes

$$\Phi_0(x,z) = -\left(0.026\ \text{cm}^{-1}\right)x + \left(0.0929\ \text{cm}^{-2}\right)x^2 + \left(0.0914\ \text{cm}^{-2}\right)z^2. \quad (10)$$

Note that, in (10), there is a term linear in x that arises from the offset error and is missing in the ideal case of (8). The phase solution now has a slight tilt and asymmetry.

The theoretical Gaussian intensity at the observation plane is again compared with the reconstructed amplitude obtained from the irradiance moment technique (Fig. 5). A phasefront solution and reconstructed intensity were also obtained by applying the iteration method algorithm to the same data. The iteration method intensity profile is shown for comparison.

Although the beam that is reconstructed using the irradiance moment algorithm has little width distortion, it does shift in the positive x-direction, albeit by a small amount. To understand the reason this shifting occurs in the irradiance moment phasefront solution, each moment must be examined. As mentioned earlier, the second-order moments do not change with the addition of an offset error. The first-order moment polynomial fits, on the other hand, are altered when an offset error occurs at one or more planes. In this case, the M_{10} (40 cm) moment increases to 0.7 cm due to the x-direction shift in the beam centroid at that plane.

The reconstructed profile from the iteration method in Fig. 5 is shifted more noticeably in the $+x$-direction and the width more distorted than the irradiance moment reconstructed profile. The shift arises from a tilt introduced in the phasefront solution at the initial plane as part of the iteration algorithm's attempt to compensate for the offset plane. The width distortion arises from the ellipticity of the beam seen by viewing the superposition of nonconcentric circles. In addition, more noise is present due to the fact that the algorithm has difficulty converging to a unique solution for this case. In fact, for offset measurement errors greater than three wavelengths, the iteration algorithm does not converge at all.

C. Gaussian Beam With Corrected Offset Measurement Error

Although the results of the previous case including offset measurement error are not dramatically different from the ideal case, it is possible to correct these errors by examining the moments. This error-correcting feature of the irradiance moment technique is its main advantage over other phase-retrieval methods. For example, the M_{10} moment at $y = 40$ is easily identified as measurement error since it is not physically possible for the beam centroid to travel in a path other than a straight line. The intensity at this plane may be shifted in the $-x$-direction such that the M_{10} (40 cm) moment is aligned with the other four moments. The phase retrieved by the irradiance moment approach in this corrected case reverts back to the original solution obtained using the ideal Gaussian beam [see (8)].

It is also possible to improve the irradiance moment phase solution by selective data omission. If the $y = 40$ cm plane is not included in the data set, only four planes are used to retrieve the phase. These four planes, however, will still be able to produce the ideal Gaussian second-order polynomial phasefront solution since the data set will now lack measurement error.

V. Irradiance Moment Technique Results: Cold-Test Gyrotron Data

The irradiance moment approach is further explored by testing the algorithm with measured gyrotron intensity data. Namely, the input is taken from the cold test results of a 1-MW 110-GHz gyrotron built by Communications and Power Industries (CPI), Palo Alto, CA. The discretely sampled data form a set of eight intensity measurements at various locations from the window $y = -10, -5, 0, 5, 10, 20, 40, 60$ cm (Fig. 6). The paraxial beam radiated by the internal mode converter (see Fig. 1) is centered at $(x, z) = (0\ \text{cm}, 37.4\ \text{cm})$, which is on axis with the window center.

In principle, a seventh-order polynomial phase expansion may be applied to the algorithm since eight planes are available. However, the phasefront is only expanded to fourth-order $(N = 4)$ to simplify the system to a set of 14 equations [see (7)]. In addition, the accuracy of a seventh-order polynomial moment fit, which would be required for a seventh-order 2-D phasefront solution, would be limited using only eight data planes.

To find the solution to a unique fourth-order 2-D phase expansion with the irradiance moment approach requires at least $N + 1$ or five planes. To obtain accurate polynomial fits of the various moments, the first seven planes are used in the calculations. The phase is retrieved at the initial ($y = -10$ cm) plane by fitting each moment to an appropriate polynomial in y using the seven planes. It is convenient here to reserve the final $y = 60$ cm plane as the observation or check plane.

After the initial phase is constructed, the approximated wave function may then be propagated from the $y = -10$ cm plane using the measured initial intensity and the 2-D phasefront expansion computed from the irradiance moment technique. To test the accuracy of the solution computed by the fourth-order irradiance moment scheme, the beam is advanced to the observation plane $y = 60$ cm. A normalized error E is then calcu-

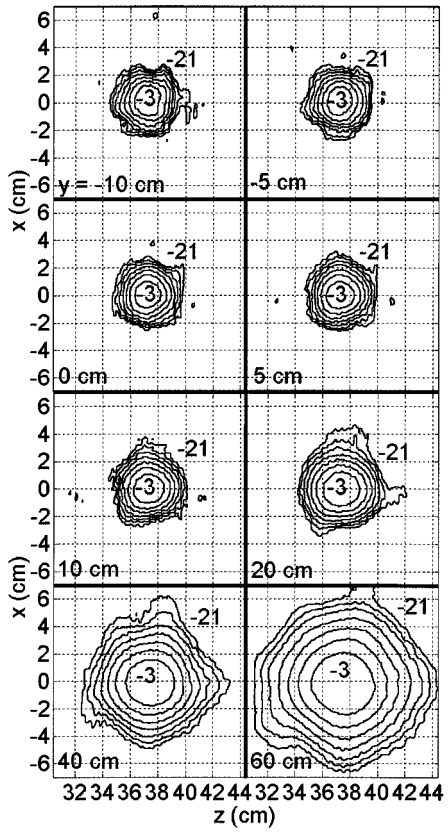

Fig. 6. Contour intensities of the eight measurement planes are shown from the CPI gyrotron in a cold test. The window center is at $z = 37.4$ cm, $x = 0$ cm. Contours of constant intensity are at 3-dB intervals from peak. All axial distances y are referenced from the window plane.

lated between the method's computed amplitude $A_y^{(c)}(x,z)$ and the measured amplitude $A_y^{(m)}(x,z)$ at this plane

$$E = 1 - \frac{\left|\int\int dx\,dz A_y^{(c)}(x,z) A_y^{(m)}(x,z)\right|^2}{\int\int dx\,dz \left|A_y^{(c)}(x,z)\right|^2 \int\int dx\,dz \left|A_y^{(m)}(x,z)\right|^2}. \tag{11}$$

Applying the error equation to the beam that was reconstructed from the irradiance moment technique, we find $E = 0.019$ at $y = 60$ cm. Using the same data in the iteration method algorithm, the error E is 0.015. Both methods yield a very small error at the observation plane, with the iteration method error somewhat smaller than the error from the irradiance moment approach. While this result is not immediately obvious in a comparison of the reconstructed intensity contour plots at $y = 60$ cm (Fig. 7), the intensity profiles along the x transverse direction shown in Fig. 8 demonstrate that the irradiance moment phasefront solution predicts a slightly narrower beam at the observation plane than measured.

The reason the reconstructed beam has a narrower waist than expected (Fig. 8) may be explained by the second-order moments, which indicate the beam size. The quadratic fit of M_{20}, for example, if extended to the observation plane, predicts a lower moment value than the moment value of the measured intensity pattern. The reason for this discrepancy is small measurement errors.

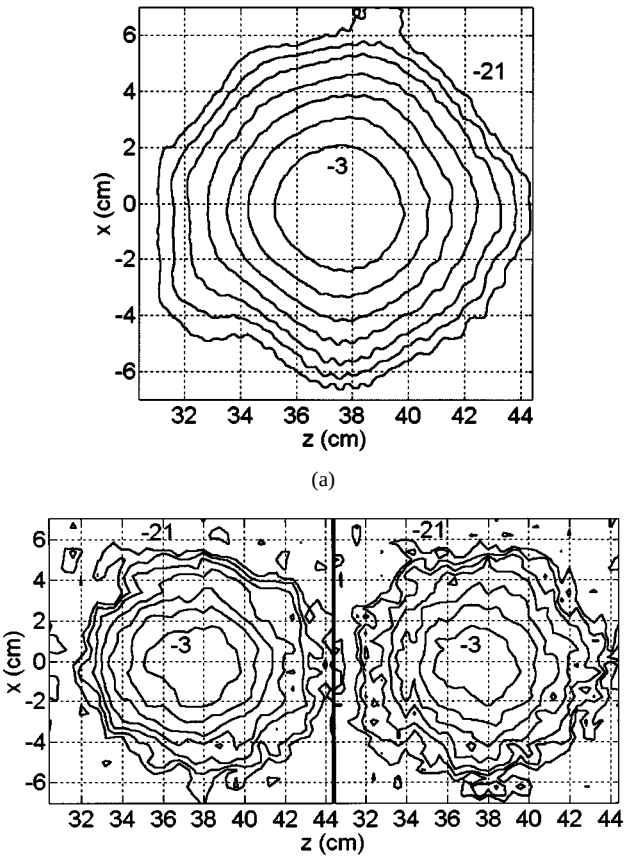

(a)

(b)

Fig. 7. (a) Measured intensity contour plot at the observation plane $y = 60$ cm. The left half of (b) is the reconstructed intensity using the irradiance moment approach and the right half is the reconstructed intensity using the iteration method.

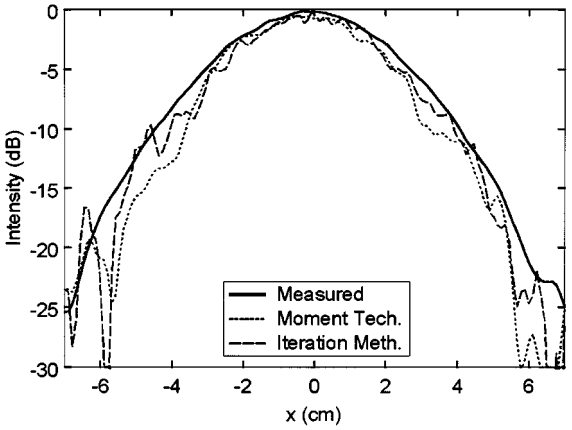

Fig. 8. $y = 60$ cm profile at mid-plane is shown along x for the measured and reconstructed intensities.

It is evident from the first- and second-order moments in x, M_{10} and M_{20}, shown in Fig. 9, that at least some measurement error has occurred since the seven first-order moments do not precisely follow a linear fit and the seven second-order moments do not follow a perfect quadratic fit. This error is reflected by experimental inaccuracies in both the beam drift and size at several (or all) planes. These measurement errors limit the overall accuracy of the moment-method phasefront solution.

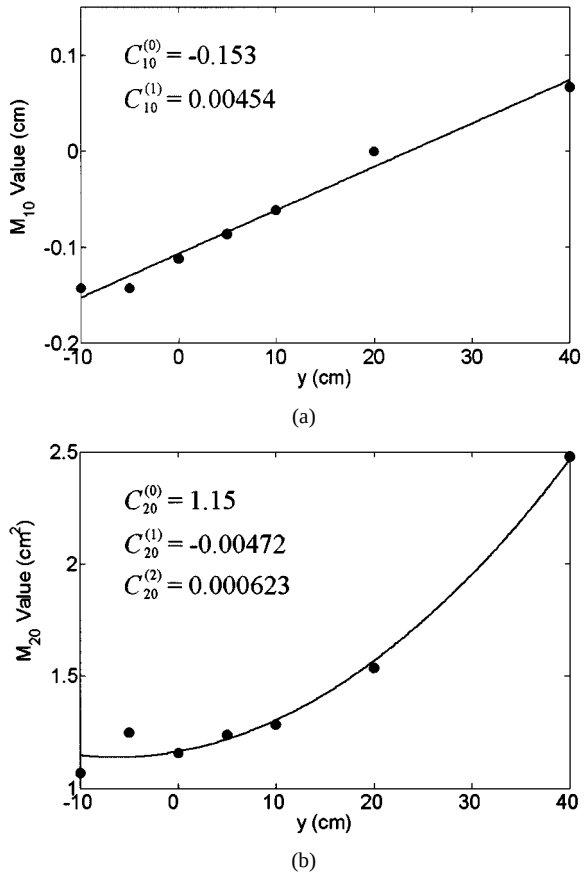

Fig. 9. Beam centroid $\langle x \rangle$ is plotted versus propagation distance y in (a) and the beam size $\langle x^2 \rangle$ is plotted versus y in (b). These points must lie on a straight line and quadratic, respectively, with the deviation indicating experimental error.

It should be mentioned that the results obtained by the irradiance moment algorithm may also be improved if the 2-D phasefront solution is expanded to fifth or sixth order. While the measurement errors would not be reduced, the addition of higher order aberrations could compensate for these inaccuracies. Such approaches, however, would require increasingly large and cumbersome sets of equations. The effectiveness of adding higher order terms to the phasefront expansion is questionable.

VI. Conclusion

The theory and general method for retrieving the phase of gyrotron beams based on weighted amplitude moments has been presented. In addition, the success of this moment method has been demonstrated by testing the algorithm with an ideal Gaussian beam, a Gaussian beam with one offset plane, and with measured data. Furthermore, the irradiance moment approach has been benchmarked against the previously developed iteration method. The amplitude errors produced from the irradiance moment approach were comparable with those from the iteration method in each case even without error correction.

The main advantage of the phase-retrieving irradiance moment technique is its ability to locate and compensate for significant measurement errors. In addition, the irradiance moment approach produces an analytical solution and eliminates the need for computationally intensive iterative calculations to produce accurate results.

As discussed in this paper, the irradiance moment technique is a powerful tool for determining the accuracy of the images used in a phase-retrieval analysis. In this paper, the example of a gyrotron cold test beam was found to have relatively small errors. In that case, the retrieved phase is quite accurate. There is very little improvement in accuracy, if any, to be gained by attempting to reject data planes that are slightly misaligned. In previous work on external phase correcting mirrors for a gyrotron in use at the large helical device (LHD) stellarator, National Institute for Fusion Science, Toki, Japan, we found that a large improvement was possible if planes that were out of alignment were rejected. That work is described in [15].

While initial results indicate the effectiveness of the irradiance moment approach, modifications may be made to enhance the algorithm and improve its performance. A nonlinear approach to solving the phase coefficients may increase the accuracy of the solution. This nonlinear irradiance moment technique would require the moment coefficients of higher rank discarded in the linear version. Finally, an "iterative irradiance moment method" may be developed, which incorporates ideas from both phase-retrieval algorithms. These topics could be the subject of future research.

The present examples show that the irradiance moment technique, previously limited to phase-retrieval problems in the optical regime, can be successfully applied to retrieving the phase of microwave beams. It is a promising new approach to an old problem. This method may become a novel and powerful numerical method to predicting gyrotron beam behavior and shaping phase-correcting mirrors. However, further research is needed to estimate the accuracy of the technique, including research on random noise, more complex measurement errors, and beams with more complex amplitude forms.

Appendix
First- and Second-Order Moments

Here, we will present an example of the irradiance moment technique using the first- and second-order moments. After the moments are expanded in terms of the initial phase, the initial phasefront is expanded and substituted into the expressions. Finally, the linear set of equations is obtained after the phasefront is properly truncated.

Deriving explicit expressions for the moments is straightforward. The first- and second-order moments $(p+q) \leq 2$ are as follows [from (2)]:

$$
\begin{aligned}
M_{10}(y) &= \langle x \rangle \\
&= M_{10}(0) - \frac{y}{k} \int\int dx\, dz \frac{\partial \Phi_0}{\partial x} A_0^2(x,z) \\
M_{01}(y) &= \langle z \rangle \\
&= M_{01}(0) - \frac{y}{k} \int\int dx\, dz \frac{\partial \Phi_0}{\partial z} A_0^2(x,z) \\
M_{20}(y) &= \langle x^2 \rangle \\
&= M_{20}(0) - 2\frac{y}{k} \int\int dx\, dz \left[x \frac{\partial \Phi_0}{\partial x} A_0^2 \right] \\
&\quad + \frac{y^2}{k^2} \int\int dx\, dz \left[\left(\frac{\partial A_0}{\partial x} \right)^2 + A_0^2 \left(\frac{\partial \Phi_0}{\partial x} \right)^2 \right]
\end{aligned}
$$

$$
\begin{aligned}
M_{11}(y) &= \langle xz \rangle \\
&= M_{11}(0) - \frac{y}{k}\int\int dx\,dz \left[x\frac{\partial \Phi_0}{\partial z}A_0^2 + z\frac{\partial \Phi_0}{\partial x}A_0^2 \right] \\
&\quad + \frac{y^2}{k^2}\int\int dx\,dz \frac{\partial \Phi_0}{\partial x}\frac{\partial \Phi_0}{\partial z}A_0^2 \\
M_{02}(y) &= \langle z^2 \rangle \\
&= M_{02}(0) - 2\frac{y}{k}\int\int dx\,dz \left[z\frac{\partial \Phi_0}{\partial z}A_0^2 \right] \\
&\quad + \frac{y^2}{k^2}\int\int dx\,dz \left[\left(\frac{\partial A_0}{\partial z}\right)^2 + A_0^2\left(\frac{\partial \Phi_0}{\partial z}\right)^2 \right].
\end{aligned}
$$

Note that, by definition, $M_{00}(0) = 1$. By generalizing and renaming the coefficients $C_{pq}^{(m)}$ [see (4)], these five moments are restated as

$$
\begin{aligned}
M_{10}(y) &= C_{10}^{(0)} + C_{10}^{(1)} y \\
M_{01}(y) &= C_{01}^{(0)} + C_{01}^{(1)} y \\
M_{20}(y) &= C_{20}^{(0)} + C_{20}^{(1)} y + C_{20}^{(2)} y^2 \\
M_{11}(y) &= C_{11}^{(0)} + C_{11}^{(1)} y + C_{11}^{(2)} y^2 \\
M_{02}(y) &= C_{02}^{(0)} + C_{02}^{(1)} y + C_{02}^{(2)} y^2.
\end{aligned}
$$

The moment coefficients required for the irradiance moment algorithm $C_{pq}^{(0)}$ and $C_{pq}^{(1)}$ are determined from the data by fitting each moment to its appropriate polynomial.

Continuing our example, the following are expressions for the linear $(m = 1)$ moment coefficients of the moments M_{pq}, where $(p + q) \leq 2$ [also derivable from (5)]:

$$
\begin{aligned}
C_{10}^{(1)} &= -\frac{1}{k}\int\int dx\,dz \frac{\partial \Phi_0}{\partial x}A_0^2 \\
C_{01}^{(1)} &= -\frac{1}{k}\int\int dx\,dz \frac{\partial \Phi_0}{\partial z}A_0^2 \\
C_{20}^{(1)} &= -\frac{2}{k}\int\int dx\,dz \left[x\frac{\partial \Phi_0}{\partial x}A_0^2 \right] \\
C_{11}^{(1)} &= -\frac{1}{k}\int\int dx\,dz \left[x\frac{\partial \Phi_0}{\partial z}A_0^2 + z\frac{\partial \Phi_0}{\partial x}A_0^2 \right] \\
C_{02}^{(1)} &= -\frac{2}{k}\int\int dx\,dz \left[z\frac{\partial \Phi_0}{\partial z}A_0^2 \right].
\end{aligned}
$$

By substituting the 2-D polynomial expansion for the phase [see (6)], the linear moment coefficients in our example become

$$
\begin{aligned}
C_{10}^{(1)} &= -\frac{1}{k}\left[\phi_{10}\int\int dx\,dz A_0^2 + 2\phi_{20}\int\int dx\,dz \left(xA_0^2\right) \right. \\
&\qquad \left. + \phi_{11}\int\int dx\,dz \left(zA_0^2\right) + \cdots \right] \\
C_{01}^{(1)} &= -\frac{1}{k}\left[\phi_{01}\int\int dx\,dz A_0^2 + \phi_{11}\int\int dx\,dz \left(xA_0^2\right) \right. \\
&\qquad \left. + 2\phi_{02}\int\int dx\,dz \left(zA_0^2\right) + \cdots \right] \\
C_{20}^{(1)} &= -\frac{2}{k}\left[\phi_{10}\int\int dx\,dz \left(xA_0^2\right) + 2\phi_{20}\int\int dx\,dz \left(x^2A_0^2\right) \right. \\
&\qquad \left. + \phi_{11}\int\int dx\,dz \left(xzA_0^2\right) + \cdots \right] \\
C_{11}^{(1)} &= -\frac{1}{k}\left[\phi_{10}\int\int dx\,dz \left(zA_0^2\right) + \phi_{01}\int\int dx\,dz \left(xA_0^2\right) \right. \\
&\qquad + 2\phi_{20}\int\int dx\,dz \left(xzA_0^2\right) \\
&\qquad + \phi_{11}\int\int dx\,dz (x^2+z^2)A_0^2 \\
&\qquad \left. + 2\phi_{02}\int\int dx\,dz \left(xzA_0^2\right) + \cdots \right] \\
C_{02}^{(1)} &= -\frac{2}{k}\left[\phi_{01}\int\int dx\,dz \left(zA_0^2\right) + \phi_{11}\int\int dx\,dz \left(xzA_0^2\right) \right. \\
&\qquad \left. + 2\phi_{02}\int\int dx\,dz \left(z^2A_0^2\right) + \cdots \right].
\end{aligned}
$$

Recognizing that the integrations in the equations relating $C_{pq}^{(1)}$ to the initial phase are the moments at the initial plane, the coefficients can be restated as follows:

$$
\begin{aligned}
C_{10}^{(1)} &= -\frac{1}{k}\left[\phi_{10} + 2\phi_{20}M_{10}(0) + \phi_{11}M_{01}(0) + \cdots \right] \\
C_{01}^{(1)} &= -\frac{1}{k}\left[\phi_{01} + \phi_{11}M_{10}(0) + 2\phi_{02}M_{01}(0) + \cdots \right] \\
C_{20}^{(1)} &= -\frac{2}{k}\left[\phi_{10}M_{10}(0) + 2\phi_{20}M_{20}(0) + \phi_{11}M_{11}(0) + \cdots \right] \\
C_{11}^{(1)} &= -\frac{1}{k}\left[\phi_{10}M_{01}(0) + \phi_{01}M_{10}(0) + 2\phi_{20}M_{11}(0) \right. \\
&\qquad \left. + \phi_{11}(M_{20}(0) + M_{02}(0)) + 2\phi_{02}M_{11}(0) + \cdots \right] \\
C_{02}^{(1)} &= -\frac{2}{k}\left[\phi_{01}M_{01}(0) + \phi_{11}M_{11}(0) + 2\phi_{02}M_{02}(0) + \cdots \right].
\end{aligned}
$$

A further simplification may be made by substituting in the coefficients of zero rank in place of the moments at the initial plane since, from (4), $C_{pq}^{(0)} = M_{pq}(0)$. Finally, the phasefront is truncated to the appropriate order, in this case, $(p+q)_{\max} = (i+j)_{\max} = N = 2$. The set of equations then becomes

$$
\begin{aligned}
C_{10}^{(1)} &= -\frac{1}{k}\left[\phi_{10} + 2\phi_{20}C_{10}^{(0)} + \phi_{11}C_{01}^{(0)} \right] \\
C_{01}^{(1)} &= -\frac{1}{k}\left[\phi_{01} + \phi_{11}C_{10}^{(0)} + 2\phi_{02}C_{01}^{(0)} \right] \\
C_{20}^{(1)} &= -\frac{2}{k}\left[\phi_{10}C_{10}^{(0)} + 2\phi_{20}C_{20}^{(0)} + \phi_{11}C_{11}^{(0)} \right] \\
C_{11}^{(1)} &= -\frac{1}{k}\left[\phi_{10}C_{01}^{(0)} + \phi_{01}C_{10}^{(0)} + 2\phi_{20}C_{11}^{(0)} \right. \\
&\qquad \left. + \phi_{11}\left(C_{20}^{(0)} + C_{02}^{(0)}\right) + 2\phi_{02}C_{11}^{(0)} \right] \\
C_{02}^{(1)} &= -\frac{2}{k}\left[\phi_{01}C_{01}^{(0)} + \phi_{11}C_{11}^{(0)} + 2\phi_{02}C_{02}^{(0)} \right].
\end{aligned}
$$

This set of equations is linear and solvable. After the moment coefficients $C_{pq}^{(0)}$ and $C_{pq}^{(1)}$ are computed from the data, the phase coefficients $\phi_{10}, \phi_{01}, \phi_{20}, \phi_{11}$, and ϕ_{02}, which describe the initial parabolic phasefront, are then easily obtainable.

ACKNOWLEDGMENT

The authors wish to thank Dr. S. Chu, Communications and Power Industries (CPI), Palo Alto, CA, for providing helpful information. The authors also acknowledge the reviewers of this paper's manuscript for very useful comments.

REFERENCES

[1] S. N. Vlasov, L. I. Zagryadskaya, and M. I. Petelin, "Transformation of a whispering gallery mode, propagating in a circular waveguide, into a beam of waves," *Radio Eng. Electron. Phys.*, vol. 12, no. 10, pp. 14–17, 1975.

[2] G. G. Denisov, A. N. Kuftin, V. I. Malygin, N. P. Venediktov, D. V. Vinogradov, and V. E. Zapevelov, "110 GHz gyrotron with built-in high-efficiency converter," *Int. J. Electron.*, vol. 72, no. 5, 6, pp. 1079–1091, 1992.

[3] K. Felch, M. Blank, P. Borchard, T. S. Chu, J. Feinstein, H. R. Jory, J. A. Lorbeck, C. M. Loring, Y. M. Mizuhara, J. M. Neilson, R. Schumacher, and R. J. Temkin, "Long-pulse and CW tests of a 110-GHz gyrotron with an internal, quasioptical mode converter," *IEEE Trans. Plasma Sci.*, vol. 24, pp. 558–569, June 1996.

[4] B. M. Harper, J. A. Lorbeck, and R. J. Vernon, "Design of an internal beam shaping system of reflectors for use in a 110 GHz $\mathrm{TE}22,6$ mode gyrotron," in *20th Int. Infrared Millimeter Waves Conf. Dig.*, Lake Buena Vista, FL, 1995, pp. 283–284.

[5] M. Blank, K. Kreischer, and R. J. Temkin, "Theoretical and experimental investigation of a quasi-optical mode-converter for a 110-GHz gyrotron," *IEEE Trans. Plasma Sci.*, vol. 24, pp. 1058–1066, June 1996.

[6] D. R. Denison, T. S. Chu, M. A. Shapiro, and R. J. Temkin, "Gyrotron internal mode converter reflector shaping from measured field intensity," *IEEE Trans. Plasma Sci.*, vol. 27, pp. 512–519, Apr. 1999.

[7] R. W. Gerchberg and W. O. Saxton, "A practical algorithm for the determination of phase from image and diffraction plane pictures," *Optik*, vol. 35, no. 2, pp. 237–246, 1972.

[8] B. Z. Katsenelenbaum and V. V. Semenov, "Synthesis of phase correctors shaping a specified field," *Radio Eng. Electron. Phys.*, vol. 12, pp. 223–230, 1967.

[9] A. V. Chirkov, G. G. Denisov, and N. L. Aleksandrov, "3D wavebeam field reconstruction from intensity measurements in a few cross sections," *Opt. Commun.*, vol. 115, pp. 449–452, 1995.

[10] A. P. Anderson and S. Sali, "New possibilities for phaseless microwave diagnostics, Part 1: Error reduction techniques," *Proc. Inst. Elect. Eng.*, pt. H, vol. 132, pp. 291–298, Aug. 1985.

[11] J. R. Fienup, "Phase retrieval algorithms: A comparison," *Appl. Opt.*, vol. 21, no. 15, pp. 2758–2769, 1982.

[12] A. A. Bogdashov, A. V. Chirkov, G. G. Denisov, D. V. Vinogradov, A. N. Kuftin, V. I. Malygin, and V. E. Zapevalov, "Mirror synthesis for gyrotron quasioptical mode converters," *Int. J. Infrared Millim. Waves*, vol. 16, no. 4, pp. 735–744, 1995.

[13] Y. Hirata, M. Komura, Y. Mitsunaka, K. Hayashi, S. Sasaki, Y. Kannai, S. Kubo, T. Shimozuma, M. Sato, Y. Takita, K. Ohkubo, and T. Watari, "Experimental coupling efficiency of shaping mirrors matching a 168-GHz gyrotron output wave to the $\mathrm{HE}11$ mode," *IEEE Trans. Microwave Theory Tech.*, vol. 47, pp. 1522–1527, Aug. 1999.

[14] H. Jory, P. Borchard, P. Cahalan, S. Cauffman, S. Chu, D. Denison, K. Felch, J. Lohr, M. Mizuhara, and D. Ponce, "Recent activities with CPI gyrotrons for ECRH," in *2nd Europhys. RF Heating Current Drive Fusion Device Topical Conf.*, Switzerland, 1998, pp. 257–60.

[15] M. A. Shapiro, T. S. Chu, D. R. Denison, M. Sato, T. Shimozuma, and R. J. Temkin, "Design of correcting mirrors for a gyrotron used at large helical device," *Fusion Eng. Des.*, vol. 53, pp. 537–544, 2001.

[16] M. R. Teague, "Irradiance moments: Their propagation and use for unique retrieval of phase," *J. Opt. Soc. Amer.*, vol. 72, no. 9, pp. 1199–1209, Sept. 1982.

[17] A. E. Siegman and S. W. Townsend, "Output beam propagation and beam quality from a multimode stable-cavity laser," *IEEE J. Quantum Elect.*, vol. 29, pp. 1212–1217, Apr. 1993.

[18] D. Marcuse, *Light Transmission Optics*, 2nd ed. New York: Van Nostrand, 1982.

[19] S. N. Vlasov, V. A. Petrishchev, and V. I. Talanov, "Averaged description of wave beams in linear and nonlinear media (moment method)," *Izv. Vyssh. Uchebn. Zaved. Radiofiz.*, vol. 14, no. 9, pp. 1353–1363, Sept. 1971.

[20] S. N. Vlasov and V. I. Talanov, *Wave Self-Focusing*. Nizhny Novgorod, Russia: Inst. Appl. Phys., Russian Acad. Sci., 1997.

[21] V. A. Borovikov, *Uniform Stationary Phase Method*, London, U.K.: IEE, 1994.

James P. Anderson received the B.S. degree in electrical engineering from the University of Wisconsin–Madison, in 1995, the M.S. degree in electrical engineering from the University of Maryland at College Park, in 1997, and is currently working toward the Ph.D. degree in electrical engineering at the Massachusetts Institute of Technology, Cambridge.

His research concerned novel electromagnetic cavity designs for high-power gyroklystron amplifiers. His current research concerns quasi-optical-mode converters and experimental research on high-power gyrotron oscillators

Michael A. Shapiro received the Ph.D. degree in radiophysics from the University of Gorky, Gorky, Russia, in 1990.

In 1995, he joined the MIT Plasma Science and Fusion Center, Massachusetts Institute of Technology, Cambridge, where he is currently a Research Scientist. His research interests include gyrotron devices, high gradient accelerators, and quasi-optics.

Richard J. Temkin (M'87–F'94) received the B.A. degree in physics from Harvard University, Cambridge, MA, in 1966, and the Ph.D. degree in physics from the Massachusetts Institute of Technology (MIT), Cambridge, in 1971.

From 1971 to 1974, he was a Post-Doctoral Research Fellow with the Division of Engineering and Applied Physics, Harvard University. Since 1974, he has been with MIT, initially with the Francis Bitter National Magnet Laboratory and then with the MIT Plasma Science and Fusion Center (PSFC) and Department of Physics. He is currently a Senior Scientist with the Physics Department, and Associate Director and Head of the Waves and Beams Division, PSFC. His research interests include novel vacuum electron devices such as the gyrotron and free electron laser, advanced high-gradient electron accelerators, quasi-optical waveguides and antennas at millimeter wavelengths, plasma heating, and electron spin resonance spectroscopy. He has authored or co-authored over 200 journal papers and book chapters. He has edited six books and conference proceedings.

Dr. Temkin is a Fellow of American Physical Society and the Institute of Physics. He was the recipient of the Kenneth J. Button Prize, the Medal of The Institute of Physics, and the Robert L. Woods Award presented by the Department of Defense for Excellence in Vacuum Electronics Research.

Douglas R. Denison received the B.S. and M.S. degrees in electrical engineering from the University of Alabama, Tuscaloosa, in 1992 and 1994, respectively, and the Ph.D. degree in electrical engineering from the Massachusetts Institute of Technology, Cambridge, in 1999.

Since 1999, he has been a Research Engineer with the Signature Technology Laboratory, Georgia Institute of Technology, Atlanta. His research interests include antenna theory, periodic structures, and numerical methods in electromagnetics.